

Steady Aerodynamic Characteristics of a Wing Flying Over a Nonplanar Ground Surface Part I: Rail

Cheolheui Han*

*School of Mechanical Engineering, Hanyang University,
Seoul 133-791, Korea*

Hakki Kim

*Graduate School of Aerospace Engineering, Hanyang University,
Seoul 133-791, Korea*

Jinsoo Cho

*School of Mechanical Engineering, Hanyang University,
Seoul 133-791, Korea*

The aerodynamic interaction between a wing and a rail is investigated using a boundary-element method. The source and doublet singularities are distributed on the wing and its guide-way rail surface. The unknown strengths of the singularities are determined by inverting the aerodynamic influence coefficient matrices. Present method is validated by comparing computed results with the other numerical data. Rail width and rail height affect the aerodynamic characteristics of the wing only if the rail is narrower than the wing span. Although the present results are limited to the inviscid, irrotational flows, it is believed that the present method can be applied to the conceptual design of the high speed ground transporters moving over the rail.

Key Words : Wing In Ground Effect, Boundary Element Method, Nonplanar Surface, Rail

Nomenclature

Roman Symbols

AR : Aspect ratio

b : Wing span, m

c : Chord length, m

C_L : Lift coefficient

C_{Di} : Induced drag coefficient

C_M : Pitching-moment coefficient

C_p : Pressure coefficient

f : Rail height, m

h : Distance between the wing's trailing edge
and the top surface of the rail, m

t : Rail half width, m

Greek Symbols

α : Angle of attack (A.O.A.), degree

Φ : Velocity potential

1. Introduction

For many centuries man has tried to travel over the world at ever increasing speeds. New concepts have been introduced to make the speed increase possible. Some of them became successful by developing new technologies to overcome obstacles. Recently, there have been worldwide efforts to develop new conceptual vehicles, focused on increasing efficiency and economy of shipping operation by using the ground effect.

For sea transporters, the viscous drag due to water friction is the main cause of the excessive power and the slower speed than the air transporters. Thus, with the conventional marine crafts, it is unlikable to operate at a high speed with acceptable fuel efficiency. The hydrofoils, hovercraft and surface effect ships are those new concepts to increase speed and fuel efficiency by

* Corresponding Author,

E-mail : timea@hanyang.ac.kr

TEL : +82-2-2220-0546; **FAX :** +82-2-2281-4016

School of Mechanical Engineering, Hanyang University, Seoul 133-791, Korea. (Manuscript **Received** August 16, 2005; **Revised** April 1, 2006)

reducing the water contact. However, sea state hinders the speed maximization of the hovercraft. The cavitation draws back the speed of a hydrofoil. The possible lowest drag marine vehicle would be a flying ship without any water contact. For ground transporters, the driving mechanism using the friction between the wheel and the ground or rail also hinders the speed increase.

Recently, there have been efforts to develop the over-the-ground-surface tracked wing-in-ground effect (WIG) vehicle such as Aero-Train (Kono et al., 1994; Kohama et al., 2000) and Aero-levitation Electric Vehicle (Han et al., 2005a). These fast transit ground transporters are supposed to move faster and to consume less energy than current conventional vehicles using the wing-in-ground-effect (Sankrithi, 1983). They are free from surface conditions due to the ground rigidity. They can fly faster at a very low altitude compared to the over-the-water-surface type WIG vehicles.

To develop and design such vehicles, it is necessary to understand the aerodynamic characteristics of the wing flying over the flat or nonplanar ground surface. Since the study on the WIG effect was firstly initiated at the beginning of the 20th century, relating to the take-off and landing of aircraft, there has been a wide spectrum of numerical approaches used to calculate the aerodynamic properties of wings in ground effect.

Wieselsberger (1922) first investigated the wing-in-ground effect using an image method. Early studies on the WIG effect were analytic (Tomotika et al., 1933. and Havelock, 1940). They used conformal mapping to find exact solutions. Rozhdestvensky (2000) presented mathematical models for the non-linear aerodynamics of lifting surfaces in extreme ground effect. The rapid increase in computing power makes it possible to use numerical methods in solving the aerodynamic problems of a wing in ground effect. Nuhait and Mook (1989) used an unsteady vortex lattice method to investigate the unsteady ground effect. Goez et al.(1984) performed the aerodynamic analysis of a low-aspect-ratio wing using a PANAIR-panel method. Chun and Park (1995) showed that water waves have an effect of

reducing the lift increase due to the ground effect. Hirata and Kodama (1995) used a CFD to study the ground effect of a three-dimensional wing with end plates. Zhang and Zerihan (2003) investigated a cambered, double-element, high-lift wing operating in ground effect. They showed that boundary-layer separation and the resultant loss of circulation on the main element cause a sharp reduction in the downforce on a wing with a large flap angle. Han et al.(2005b) investigated the wake shapes behind wings in formation flight.

Above approaches ranging from a simple lifting line method to complicated computational-fluid-dynamic analyses are reviewed extensively by Ollia (1980), Hooker (1989), and Rozhdestvensky (2000). However, those published literatures to date are focused mainly on the aerodynamic characteristics of wings near the flat ground or the water waves. To conceptually design the ground transportation vehicles, it is necessary to understand the aerodynamic characteristics of a wing flying over the rail. However, there have not been many papers in the published literature on the aerodynamic characteristics of a wing flying over the rail. Thus, a boundary-element method based on potential flow theory is applied to the aerodynamic analysis of a wing flying over a rail. The boundary element method has the advantage that it can solve the three-dimensional flows over the complex bodies with less computing time than other numerical methods. Its use can be extended to nonlinear problems by coupling with other numerical methods (Oh and Yang, 2004). The effect of the changes of parameters such as rail width, rail height, and wing height are investigated.

2. Boundary-Element Method

Only the idealized case of incompressible flow at infinite Reynolds number will be considered in this paper. For the flows of infinite Reynolds number, the influence of viscosity is confined to infinitely thin layers of fluid adjacent to the solid surface of the configuration or contained within wake sheets issuing either from sharp edges (e.g. classical trailing-edge wakes) or from smooth

surfaces (e.g. forebody vortices). The wake sheets correspond to physically-identifiable regions of rotational fluid which carry away the vorticity generated by viscous effects within the boundary layer on the configuration surface.

For an incompressible, irrotational and inviscid flow, the pressure can be determined uniquely and simply from the velocity field. The idealized flow outside any wake surfaces is a potential flow in which the velocity \vec{V} is the gradient of a scalar potential Φ which is governed by Laplace's equation :

$$\nabla^2 \Phi = 0 \tag{1}$$

Laplace equation is a linear differential equation and its general solution can be obtained by superposing basic solutions. Certain bodies in a flow domain could be represented by a suitable combination of point sources or point doublets. Thus, it seems plausible that a large number of singularities of small strength could be used to represent more complicated body shapes. A continuous volume distribution of singularities within the body might be a general representation. It amounts to the problem of specifying conditions on the boundary S of the domain of interest, Ω and then, the problem to be solved falls into the general class of boundary value problems. The flow region Ω and its boundaries will thus have the general appearance shown in Fig. 1. For a wing moving near the ground surface, it is common to use the image method in order to consider the ground effect. However, for a moving body inside nonplanar ground surfaces with a bump

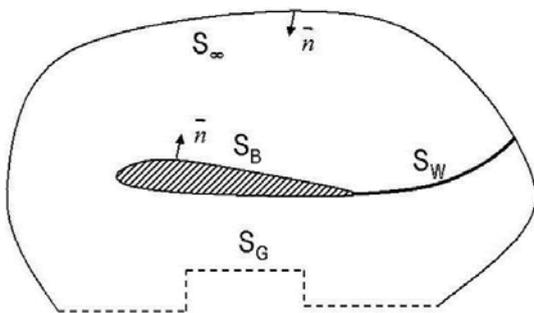


Fig. 1 Nomenclature for the flow domain and the boundary surfaces

on the ground, or the guide ways such as fence, rail and channel, it is difficult to implement the image method directly to the problems investigated. Thus, it requires another method that can model the nonplanar ground surfaces.

Consider a body with known boundaries S_B (body surface), S_W (wake surface), S_G (ground surface) and S_∞ (outer boundary) as shown in Fig. 1. The general solution to Eq. (1) can be constructed, based on Green's identity, by a sum of source σ and dipole μ distributions on all the boundaries.

$$\Phi(x, y, z) = \frac{1}{4\pi} \int_{S_B+S_W+S_G} \mu \vec{n} \cdot \nabla \left(\frac{1}{r} \right) dS - \frac{1}{4\pi} \int_{S_B+S_G} \sigma \left(\frac{1}{r} \right) dS \tag{2}$$

Imposing the Dirichlet boundary condition on the surface and using the boundary condition for an enclosed body $\partial\Phi/\partial n_B=0$, then the potential inside the body will not change. Thus, Eq. (2) results in

$$\int_{S_B+S_W+S_G} \mu \vec{n} \cdot \nabla \left(\frac{1}{r} \right) dS - \int_{S_B+S_G} \sigma \left(\frac{1}{r} \right) dS = 0 \tag{3}$$

A panel method solves a linear partial differential equation numerically by approximating the configuration surface by a set of panels on which unknown singularity strengths are defined. The body surface is approximated by a large number of small plane quadrilateral elements (N_B body surface panels, N_W additional wake panels and N_G ground surface panels), which are formed by a set of points in three-dimensional space and are given as input points. The boundary condition will be specified at each of these elements at a collocation point. Points should be distributed in such a way that they are concentrated in regions where the curvature of the body surface is large and in regions where the flow velocities are expected to change rapidly. The density of singularities is assumed constant over each of these elements. This assumption reduced the problem of determining the continuous distributions of the singularity functions to the problem of determining a finite number of values of singularities for each of the planar elements. Once the singularity strengths are established, the properties of

the flow are readily determined. Rewriting the Dirichlet boundary condition for each of the N collocation points, then (2) will have the following form :

$$\begin{aligned} & \sum_{k=1}^N \frac{1}{4\pi} \int_{bodypanel} \mu n \cdot \nabla \left(\frac{1}{r} \right) dS + \sum_{k=1}^N \frac{1}{4\pi} \int_{wakepanel} \mu n \cdot \nabla \left(\frac{1}{r} \right) dS \\ & + \sum_{k=1}^{N_c} \frac{1}{4\pi} \int_{bodypanel} \mu n \cdot \nabla \left(\frac{1}{r} \right) dS - \sum_{k=1}^N \frac{1}{4\pi} \int_{bodypanel} \sigma \left(\frac{1}{r} \right) dS \quad (4) \\ & - \sum_{k=1}^{N_c} \frac{1}{4\pi} \int_{bodypanel} \sigma \left(\frac{1}{r} \right) dS = 0 \end{aligned}$$

The integration in (4) is limited now to each individual panel element representing the influence of this panel on point P. For a unit singularity element (σ or μ), this influence depends on the panel's geometry only. The integration can be performed analytically or numerically. For a constant-strength μ element, the influence of panel k (defined by the four corners 1, 2, 3, and 4) at point P is

$$\frac{1}{4\pi} \int_{1,2,3,4} \frac{\partial}{\partial n} \left(\frac{1}{r} \right) dS |_{k=C_k} \quad (5)$$

and for a constant-strength σ element

$$-\frac{1}{4\pi} \int_{1,2,3,4} \left(\frac{1}{r} \right) dS |_{k=B_k} \quad (6)$$

These integrals are a function of the points 1, 2, 3, 4, and P. After computing the influence of each panel on each other panel, (10) for each point P inside the body becomes

$$\begin{aligned} & \sum_{k=1}^N C_{ik} \mu_k + \sum_{l=1}^{N_w} C_{il} \mu_l + \sum_{m=1}^{N_c} C_{im} \sigma_m \\ & + \sum_{k=1}^N B_{ik} \mu_k + \sum_{m=1}^{N_c} B_{im} \sigma_m = 0 \end{aligned} \quad (7)$$

Here, the source strength is defined as

$$\sigma = \vec{n} \cdot \vec{V}_\infty \quad (8)$$

where \vec{n} is the unit normal and \vec{V}_∞ is the total kinematic velocity (or onset flow) due to the motion of the arbitrary bodies.

Since the coefficients, B_k , are known, the source term can be moved to the right-hand side of the equation. The Kutta condition makes it possible to express the wake doublets in terms of the unknown surface doublets μ_k . This algebraic relation can be substituted into the C_k coefficients of the unknown surface doublet such that

$$\begin{aligned} A_k &= C_k && \text{if panel is not at T.E.} \\ A_k &= C_k \pm C_t && \text{if panel is at T.E.} \end{aligned} \quad (9)$$

where the \pm sign depends on whether the panel is at the upper or the lower side of the trailing edge. Consequently, for each collocation point P, a linear algebraic equation containing N unknown singularity variables μ_k can be derived :

$$\sum_{k=1}^N A_k \mu_k + \sum_{m=1}^{N_c} A_m \mu_m = - \left(\sum_{k=1}^N B_k \sigma_k + \sum_{m=1}^{N_c} B_m \sigma_m \right) \quad (10)$$

Evaluating (8) at each of the NT ($N+N_c$) collocation points results in NT equations with the NT unknown μ , in the following form :

$$\begin{pmatrix} a_{11} & a_{12} & \cdots & a_{1NT} \\ a_{21} & a_{22} & \cdots & a_{2NT} \\ \vdots & \vdots & \vdots & \vdots \\ a_{NT1} & a_{NT2} & \cdots & a_{NTNT} \end{pmatrix} \begin{pmatrix} \mu_1 \\ \mu_2 \\ \vdots \\ \mu_3 \end{pmatrix} = - \begin{pmatrix} b_{11} & b_{12} & \cdots & b_{1NT} \\ b_{21} & b_{22} & \cdots & b_{2NT} \\ \vdots & \vdots & \vdots & \vdots \\ b_{NT1} & b_{NT2} & \cdots & b_{NTNT} \end{pmatrix} \begin{pmatrix} \sigma_1 \\ \sigma_2 \\ \vdots \\ \sigma_3 \end{pmatrix} \quad (11)$$

The unknown strengths of the potentials are determined by inverting the aerodynamic influence coefficient matrices. The surface velocities over the wing surfaces are obtained using the potential strengths, and the surface static pressures are calculated from Bernouilli's equation. The net aerodynamic forces on the wing are calculated by integrating the pressure values over the wing's surface.

3. Results and Discussion

Figure 2 shows the nomenclature for a wing flying over a rail. The wing is assumed to cruise at the wing height of h that is the distance between the wing's trailing edge and the top surface of the rail. The rail height from the flat ground surface is represented as f . The rail half width is defined as t . Both b and c represents the wing span and the chord length, respectively.

There are not many known published data on the aerodynamic characteristics of a wing flying over the rail. Thus, the present method is validated by comparing computed results with measured data. Figure 3 shows the comparison of the present results with the measured pressure coefficient values on the centerline of a body flying in a channel (William and William, 1976). As shown in Fig. 3, the present results are in good

agreement with the measured data. Thus, it can be deduced that present method can be applied to the simulation of the wing in ground effect flying over nonplanar ground surfaces.

It has been known that Venturi effect decrease the lift of a thick wing with a symmetric airfoil section at small angles of attack near the planar ground (Han and Cho, 2000). However, the non-planar ground will affect the aerodynamic characteristics of the wing. It is assumed that two NACA wings (NACA 0006 and NACA 0015) with an aspect ratio of 1.0 and at an angle of attack of 2.0 degree are placed in close proximity

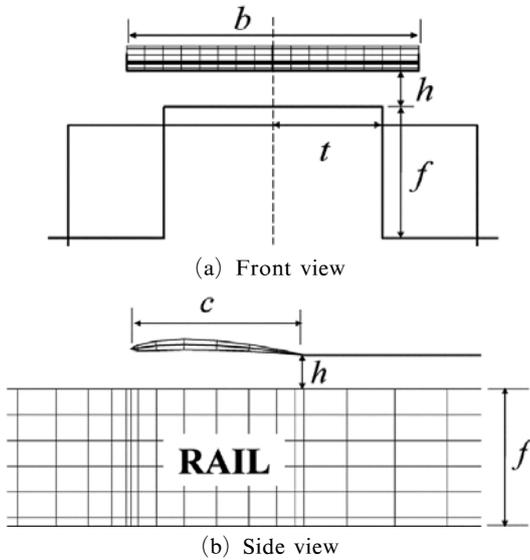


Fig. 2 Nomenclature for a wing flying over a rail

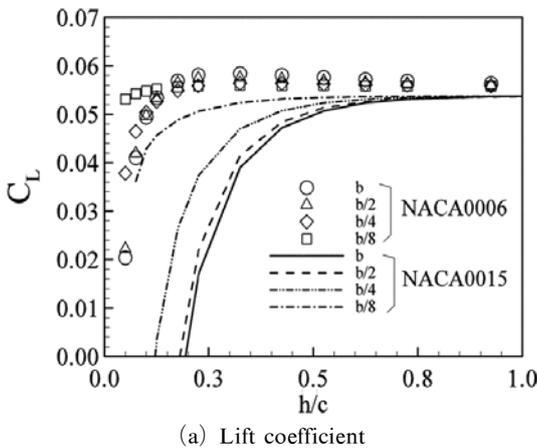


Fig. 4 Thickness effect on the aerodynamic characteristics of a wing near the rail ($\alpha=2^\circ$, $AR=1.0$, $f/c=1.0$)

to the rail. The non-dimensional rail height, f/c , is set to 1.0. In Fig. 4(a), the lift of the wings decreases due to Venturi effect. As shown in Fig. 4(b), the induced drag decreases as the wing approaches the rail top surface. It is also shown that the thick wing has the larger induced drag than the thin wing. The aerodynamic characteristics of the wings with wider wing span than the rail width do not change more than the case of the wing with narrower wingspan. It can be deduced that the air between the lower surface of the wing and the top surface of the rail can flow more easily than the air in between the wing and the flat ground.

For a wing flying at high altitude with the small or moderate range of angles of attack, the

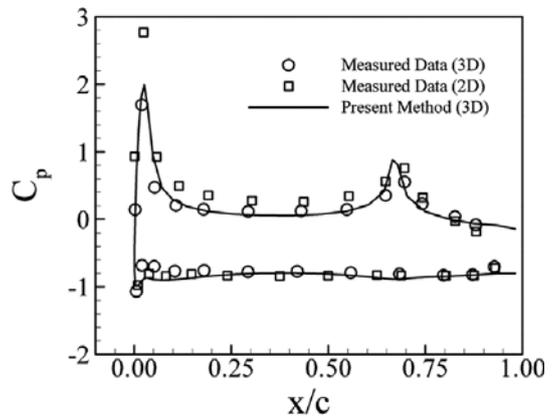


Fig. 3 Pressure coefficients on the centerline of a body flying in a channel

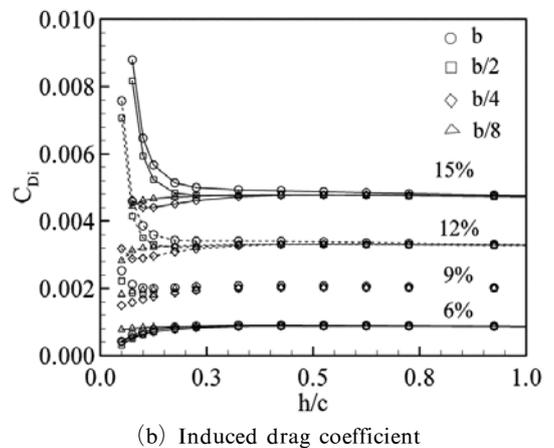


Fig. 4 Thickness effect on the aerodynamic characteristics of a wing near the rail ($\alpha=2^\circ$, $AR=1.0$, $f/c=1.0$)

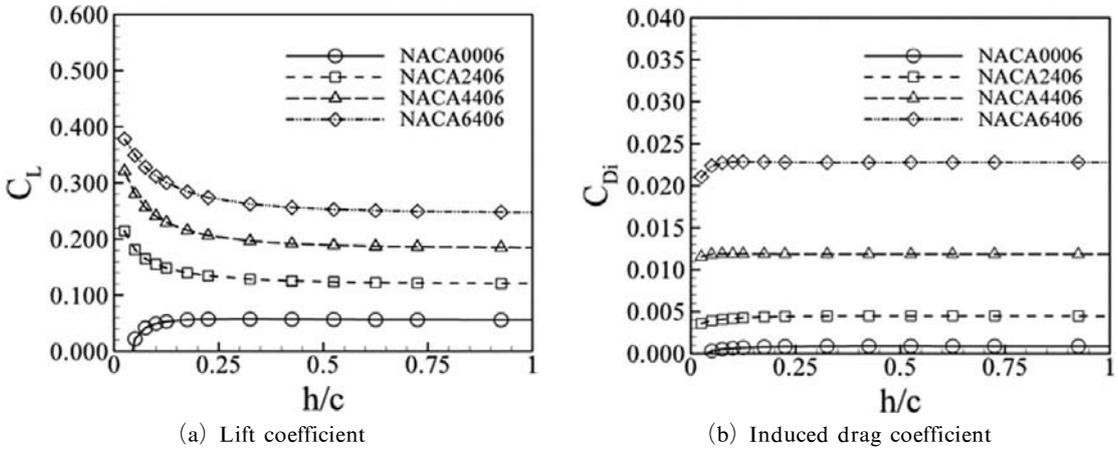


Fig. 5 Maximum camber effect on the aerodynamic characteristics of a wing for the change of the wing height ($\alpha=2^\circ$, $R=1.0$, $f/c=1.0$, $t=b/2$)

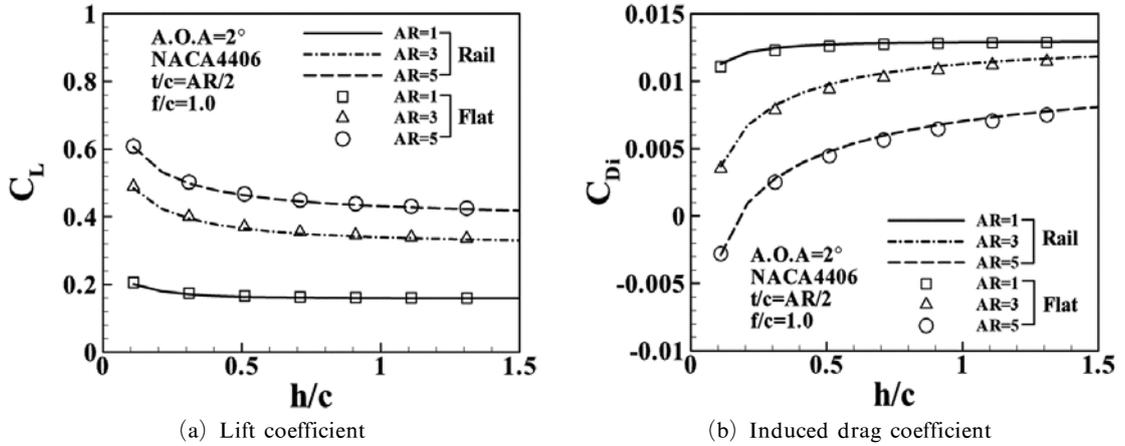


Fig. 6 Ground effect on the aerodynamic characteristics of wings with three different aspect ratios

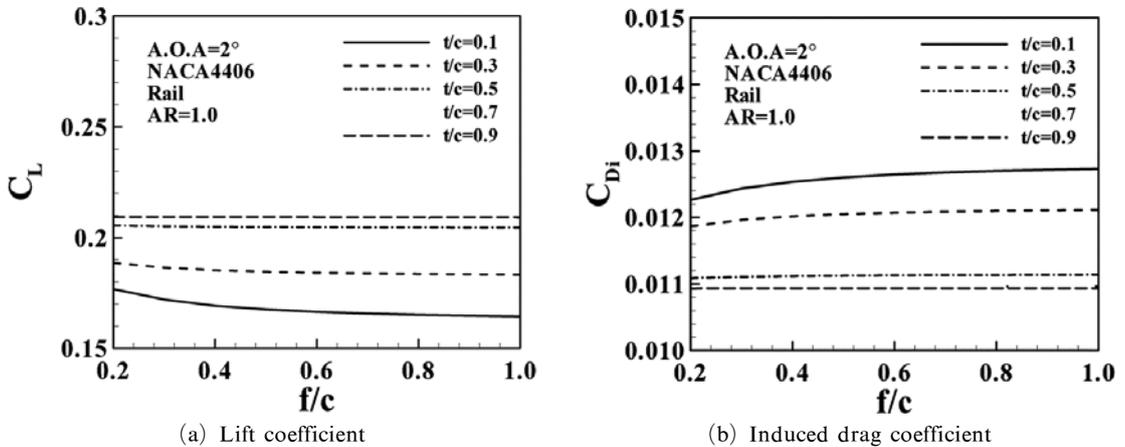


Fig. 7 Rail height effect on the aerodynamic characteristics of a wing flying at $h/c=0.1$ over the rails with different width

cambered wing has larger lift and smaller drag than the symmetric wing. Fig. 5 shows that when $h/c < 0.5$ the lift of the cambered wing increases. The induced drag decreases slightly when $h/c < 0.1$.

Figure 6 shows the effect of the aspect ratio on the aerodynamic characteristics of NACA wings flying over the rail. As shown in Fig. 6, the aerodynamic characteristics of wings flying over the rail are almost the same as those of wings moving over the flat ground. The aspect ratio has an effect of increasing the lift and decreasing the induced drag. When the rail width is equal to or larger than the wing span, the aerodynamic characteristics of a wing flying over the rail are similar to those of the wing flying over the flat ground surface.

Figure 7 shows the effect of the rail height on the aerodynamic characteristics of NACA wings flying over the rail. As shown in the figure, the rail height does not affect the aerodynamic characteristics of the wing much for $t > b/2$. When the rail is narrow ($t < b/2$), the changes in the aerodynamic characteristics of the wing due to the rail height become larger near the rail.

4. Conclusions

A study of the aerodynamic characteristics of a NACA wing flying over the rail is done using a boundary element method. Present method is validated by comparing the present result with the other numerical data. The ground effect increases the lift while decreasing the induced drag. The thickness has the effect of decreasing the lift and increasing the induced drag. The cambered wing over the rail has larger lift and smaller drag than the cambered wing over flat ground. The narrower rail than the wing span affects on the aerodynamic characteristics of the wing. The rail height does not affect the aerodynamic characteristics of the wing for the wider rail than the wing span. Although the present result is limited to the inviscid irrotational assumption, it is believed that the present method will be useful for the conceptual design of the high speed ground transporters moving over the rail.

Acknowledgments

This work was supported by Grant No. (R01-2005-000-10310-0) from the Basic Research Program of the Korean Science and Engineering Foundation. This work was also supported by Korea Research Foundation Grant funded by Korea Government (The Ministry of Education & Human Resources Development, Basic Research Promotion Fund) (KRF-2005-206-D00007).

References

- Chun, H. H. and Park, I. R., 1995, "Analysis of Steady and Unsteady Performances for 3-D Air wings in the Vicinity of the Free Surface," *Proceedings of a Workshop on Twenty-First Century Flying Ships*, edited by Prandolini, L. J., The Institute of Marine Engineers, Sidney, Australia, pp. 23~46.
- Goez, A. R., Osborn, R. F. and Smith, M. L., 1984, "Wing-In-Ground Effect Aerodynamic Predictions Using PANAIR," AIAA Paper 84-2495.
- Han, C. and Cho, J., 2000, "A Numerical Analysis of the Thickness-Induced Effect on the Aerodynamic Characteristics of Wings Moving Near Ground," *KSAS International Journal*, Vol. 1, No. 1, pp. 29~35.
- Han, C., Cho, J., Moon, Y. J., Yoon, Y. and Song, Y.K., 2005a, "Design of an Aerolevitation Electric Vehicle for High-Speed Ground Transportation System," *Journal of Aircraft*, Vol. 42, No. 1, pp. 93~104.
- Han, C., Cho, L. and Cho, J., 2005b, "Wake Shapes Behind Wings in Close Formation Flight Near the Ground," *Journal of Mechanical Science and Technology*, Vol. 19, No. 2, pp. 674~681.
- Havelock, T. H., 1940, "The Lift and Moment on a Flat Plate in a Stream of Finite Width," *Proceedings of the Royal Society of London, Series A*, Vol. 166, No. 2, pp. 19~54.
- Hirata, N. and Kodama, Y., 1995, "Flow Computation for Three-Dimensional Wing in Ground Effect Using Multi-Block Technique," *Journal of the Society of Naval Architects of Japan*, Vol. 177, pp. 49~57.

- Hooker, S. F., 1989, "A Review of Current Technical Knowledge Necessary to Develop Large Scale Wing-In-Surface Effect Craft," AIAA Paper 89-1497-CP, pp. 367~429.
- Kikuchi, K., 1997, "Numerical Simulation of the Ground Effect using the Boundary Element Method," *International Journal for Numerical Methods in FLUIDS*, Vol. 25, No. 9, pp.1043~1056.
- Kohama, Y. P., Kikichi, S., Watanabe, H., Ohta, F. and Ito, T., 2000, "Evaluation of the Transportation System in relation to Environmental Problem," *Workshop on Drag Reduction of Aircraft and Ground Transportation*, Institute of Fluid Science, Tohoku University, Sendai, Japan, pp. 12~13.
- Kono, T., Kohama, Y. and Matsui, N., 1994, "Stability of Guide Way Type Wing in Ground Effect Vehicle," *Proceedings of the third JSME-KSME Fluids Engineering Conference*, JSME, Sendai, Japan, pp. 715~718.
- Nuhait, A. O. and Mook, D. T., 1989, "Numerical Simulation of Wings in Steady and Unsteady Ground Effects," *Journal of Aircraft*, Vol. 26, No. 12, pp. 1081~1089.
- Oh, Y. K. and Yang, H. D., 2004, "A Study on Correlation between Pressure Variations and Augmentation of Heat Transfer in Acoustic Fields," *KSME International Journal*, Vol. 18, No. 9, pp. 1630~1639.
- Ollia, R. G., 1980, "Historical Review of WIG vehicles," *Journal of Hydronautics*, Vol. 12, No. 3, pp. 65~76.
- Rozhdestvensky, K. V., 2000, *Aerodynamics of a lifting system in extreme ground effect*, Springer-Verlag, Berlin, Chap. 1.
- Sankrithi, M., 1983, "The Tracked Wing In Ground-Effect," Ph. D. Dissertation, Department of Mechanical and Aerospace Engineering, Princeton University.
- Tomotika, S., Nagamiya, T., and Takenouti, Y., 1933, "The lift on a Flat Plate Placed Near a Plane Wall, with Special Reference to the Effect of Ground Upon the Lift of a Monoplane Aerofoil," Aeronautical Research Institute, Rept. 97, Tokyo Imperial Univ., Tokyo (as reported in Pistolesi, 1935).
- Wieselsberger, C., 1922, "Wing Resistance Near the Ground," *NACA TM77*.
- William, H. A. and William, R. E., 1976, "Configuration Effect on the Lift of a Body in Close Ground Proximity," *Journal of Aircraft*, Vol. 13, No. 8, pp. 584~589.
- Zhang, X. and Zerihan, J., 2003, "Aerodynamics of a Double-Element Wing in Ground Effect," *AIAA Journal*, Vol. 41, No. 6, pp. 1007~1016.